Indirect Fluorine Coupling Anisotropies in *p*-Difluorobenzene: Implications to Orientation and Structure Determination of Fluorinated Liquid Crystals

Juha Vaara,[†] Jaakko Kaski, and Jukka Jokisaari*

NMR Research Group, Department of Physical Sciences, University of Oulu, P. O. Box 3000, FIN-90401 Oulu, Finland

Received: April 20, 1999; In Final Form: May 4, 1999

The spin−spin coupling tensors, $\mathbf{J}_{XF}$ (X = H, C, F), in *p*-difluorobenzene ($C_6H_4F_2$) were determined using ab initio multiconfiguration self-consistent field linear response calculations and NMR experiments performed in nematic liquid crystal phase. The theoretical spin−spin coupling constants are in fair agreement with experimental results. By supplying the experimental data analysis with some of the results of the theoretical calculations, the remaining anisotropy and asymmetry parameters pertinent to the ${}^n\mathbf{J}_{CF}$ (n = 1, 2, 3, 4) and ${}^5\mathbf{J}_{FF}$ tensors were obtained in good agreement with the ab initio data. The results indicate that the tensorial properties of the fluorine couplings typically contribute a few percent to the corresponding experimental anisotropic couplings. In D_{2h} or lower point group symmetries, the indirect coupling can even dominate the experimental dipolar coupling because of occasional cancellation of the direct part. Consequently, the contribution of J_{XF}^{aniso} must be taken into account when using anisotropic couplings in accurate determinations of the geometry or orientation of fluorinated liquid crystals or other molecules containing fluorine-substituted phenyl rings dissolved in mesophases.

1. Introduction

In NMR experiments performed in anisotropic liquid crystal (LC) or solid phases, the contribution J_{KL}^{aniso} from the indirect spin−spin coupling tensor $\mathbf{J}_{KL}$ appears in the experimentally observable anisotropic NMR coupling, $D_{KL}^{exp} = D_{KL} + {}^1/_2 J_{KL}^{aniso}$, between the nuclei K and L.[1,2] Information on the molecular structure and orientation with respect to the external magnetic field is contained in the direct dipolar coupling, D_{KL}. Thus, J_{KL}^{aniso} should be relatively small or known when accurate structural or orientational data are wanted. For example, the one-bond couplings between carbon nuclei have negligible J_{CC}^{aniso} regardless of hybridization,[3,4] justifying the recently introduced method of obtaining the direct CC couplings at natural abundance for LC molecules using two-dimensional double-quantum experiments.[5] Likewise, for HH and CH couplings, J_{KL}^{aniso} is generally small.[1]

The idea to partially orient molecules in liquid crystalline solutions and to utilize residual dipolar couplings in structural analysis was proposed over 35 years ago.[6] Since then the method has developed to a level that renders possible very accurate molecular structure determinations. This, however, necessitates consideration of various contributions, such as molecular vibrations, correlation of vibrational and reorientational motions, and spin−spin coupling tensor, in the experimental dipolar couplings, D_{KL}^{exp}, as seen below. Recently, the utility of residual dipolar couplings in the derivation of structural information on weakly aligned biomacromolecules has been recognized, and the field is gaining growing interest.[7] When applying the technique to macromolecular systems, one should notice that most likely the system contains a bond or bonds whose order parameter is vanishingly small. If this is the case, the above-mentioned contributions may even dominate D_{KL}^{exp}, leading to errors in structural parameters. This paper deals exclusively with spin−spin coupling tensors in *p*-difluorobenzene, and consequently we aim only for the significance of the spin−spin coupling tensor in the respective D_{KL}^{exp}.

In the field of LC NMR research, ^{19}F is an important, easily observed spin = $^1/_2$ nucleus due to its 100% natural abundance. It is often used as a substituent for hydrogen, resulting in changes in the material properties. In particular, the resistivity of fluorinated LCs is high, making them suitable for display technology. Fluorine substitution enables straightforward extraction of the FF and CF dipolar couplings by proton irradiation. However, J_{KL}^{aniso} is likely to be bigger in couplings involving fluorine than in the proton or carbon couplings. On the basis of the semiempirical calculations of Haigh and Sykes,[8] particularly the ratio $J_{FF}^{aniso}/2D_{FF}$ may be up to several percent in fluorobenzenes, while the anisotropic contributions to the HF coupling have been found to be in the sub-1% range.[1]

Recently, Magnuson et al. investigated the orientational order of various LCs containing fluorine-substituted benzene rings using the CF dipolar couplings.[9] Early electronic structure calculations predict small effects due to J_{CF}^{aniso} for the CF couplings for fluoromethanes (see ref 1 for references), but no modern theoretical studies for fluorine-containing aromatic systems have been carried out. The many different contributions to the $\mathbf{J}_{KL}$ tensors, and the sensitivity to the quality of the basis set and electron correlation treatment, place stringent requirements even on the contemporary computational methods and facilities in ab initio calculations of this property.[10] Ab initio methods are, at best, able to provide unbiased predictions for the spin−spin couplings, contrary to the semiempirical methods which are often known to fail for properties and/or systems not used in their parametrization. Consequently, it has not been until recently that reliable theoretical calculations of the $\mathbf{J}_{KL}$ tensors

* To whom correspondence should be addressed. Telephone: +358-8-553 1308. Fax: +358-8-553 1287. E-mail: Jukka.Jokisaari@oulu.fi.

[†] Present address: Max-Planck-Institut für Festkörperforschung, Heisenbergstrasse 1, D-70569 Stuttgart, Germany.

10.1021/jp991295+ CCC: $18.00
Published on Web 07/03/1999

TABLE 1: Ab Initio Calculated and Experimental Geometries of *p*-Difluorobenzene[a]

method	r_{CH}	r_{CF}	r_{C7C8}[b]	r_{C8C9}[b]	∠C12−C7−C8[b]	∠H1−C8−C9[b]
MP2/cc-pVDZ	1.0933	1.3508	1.3986	1.4040	121.62	121.24
MP2/AUG-cc-pVDZ	1.0922	1.3679	1.3989	1.4074	122.68	121.35
QCISD/cc-pVDZ	1.0939	1.3508	1.3985	1.4049	121.73	121.24
extrapolated[c]	1.0929	1.3679	1.3988	1.4082	122.79	121.35
NMR/I[d]	1.0822	1.3476[e]	1.3913	1.3972	121.92	121.35
NMR/II[d]	1.0818	1. 3476[e]	1.3908	1.3973	121.99	121.30
NMR/III[d]	1.0827	1. 3476[e]	1.3917	1.3972	121.99	121.35
NMR/IV[d]	1.0826	1. 3476[e]	1.3912	1.3972	121.94	121.34
NMR/V[d]	1.0799	1. 3476[e]	1.3879	1.3941	122.16	121.38
ED[f]	1.088(5)	1.354(4)	1.388(3)	1.400(3)	123.5(1)	118.5(8)
ED[g]	1.070	1.3476	1.385	1.396	123.1	117.8

[a] Bond lengths in angstroms and angles in degrees. [b] The numbering refers to Figure 1. [c] Extrapolated geometry based on the ab initio MP2 and QCISD results. [d] Present liquid crystal NMR results for the r_α geometry at 300 K. [e] Fixed in the analysis of the present experiments. [f] Electron diffraction (r_g) results taken from ref 25. [g] The r_g geometry of footnote *f* transformed to r_α at 300 K.

have become feasible, and therefore old data should be considered with caution.

A method of determining the J_{KL}^{aniso} contributions experimentally using LC NMR is to take advantage of a combination of proper nematic solvent mixtures in order to minimize deformation effects due to anisotropic forces. In a more sophisticated approach, the deformational corrections to the couplings are calculated on the basis of the optimized interaction tensors **A** acting on the bonds of the solute.[11−13] The **A** tensors also determine the molecular orientational order parameters.[11] In both cases, the corrections for harmonic molecular vibrations[14] are also required.

To shed further light into the question of whether the J_{HF}^{aniso}, J_{CF}^{aniso}, and J_{FF}^{aniso} contributions can safely be neglected for fluorine-substituted benzenes and LCs containing fluorinated aromatic groups, we report ab initio multiconfiguration self-consistent field (MCSCF) linear response (MCLR) calculations of the corresponding coupling tensors in *p*-difluorobenzene ($C_6H_4F_2$). Also, we describe LC NMR experiments for the same system dissolved in certain nematic LC solvent mixtures, chosen to minimize deformation effects; the remaining deformation is also corrected for. The LC NMR information obtained by us is, as such, insufficient for determining the tensor components of the HF, CF, and FF couplings that affect the LC NMR spectra. However, by incorporating some of the theoretical results to the analysis of experimental data, definite conclusions can be drawn.

2. Calculations

Ab initio calculations of the $\mathbf{J}_{HF}$, $\mathbf{J}_{CF}$, and $\mathbf{J}_{FF}$ tensors were carried out for the isolated $C_6H_4F_2$ molecule using the MCLR method as implemented by Vahtras et al.[15] to the DALTON program system.[16] All the different physical mechanisms, the dia- and paramagnetic spin−orbit (DSO and PSO), the spin−dipole (SD), Fermi contact (FC), and SD/FC cross-term contributions were calculated. We refer to the original article[15] and recent review[10] for details of the theory and implementation. Instead, we focus on the role of the different approximations that limit the attainable accuracy for the present system, whose size prevents attempts of reaching undisputable convergence of ab initio calculations. We note in passing that the recently introduced density functional method[17] that otherwise is very suitable for large molecules is currently unable to provide realistic couplings to fluorine or other atoms containing lone pairs.[18,19]

The equilibrium geometry for the molecule was optimized using the Gaussian 94 program[20] at the MP2[21,22] and QCISD[23] levels with the cc-pVDZ and AUG-cc-pVDZ basis sets,[24] as shown in Table 1.

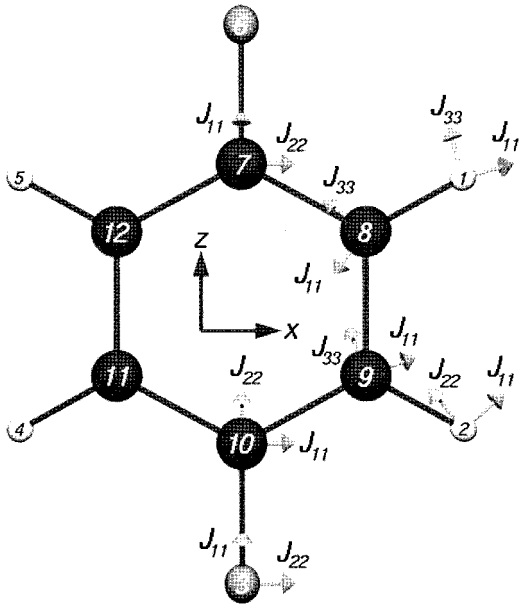

Figure 1. Numbering of nuclei and the placement of the molecule-fixed coordinate system in *p*-difluorobenzene. The directions of the principal axes of the ab initio calculated fluorine spin−spin coupling tensors are also shown. In each case, one of the coupled nuclei is the fluorine at the top of the figure, and the axes are illustrated on top of the other nucleus. For each tensor, only the two axes located in the plane of the molecule are displayed.

In the calculations of the $\mathbf{J}_{KL}$ tensors, we employed two geometries: firstly, one obtained by extrapolation of the changes caused by using the larger AUG-cc-pVDZ basis set instead of the smaller cc-pVDZ and using the better QCISD treatment of electron correlation instead of MP2; secondly, to obtain an estimate of the sensitivity of the results to the choice of geometry, we recalculated the coupling tensors also at an experimental geometry[25] using each of the MCSCF wave functions. In each geometry, the FF symmetry axis of the molecule is placed in the direction of the *z* coordinate axis, and the *y* direction is normal to the plane of the molecule. The axes and numbering of nuclei are illustrated in Figure 1.

We used two one-particle basis sets in the MCLR calculations of the $\mathbf{J}_{KL}$ tensors, the HII set adopted from refs 26 and 27 and a set that we denote as HIIs3, obtained by modifying the HII set. The HII basis is 9s5p1d/5s4p1d for C and F atoms in the primitive/contracted Gaussian type orbital notation and 5s1p/3s1p for H. Only the innermost atomic orbitals (1s and 2p) are contracted. HII contains 200 basis functions for $C_6H_4F_2$ and is of the triple-ζ plus polarization quality. This set has been employed extensively in the calculation of NMR properties, and

in a recent systematic basis set investigation[28] it was shown to perform very well for its size for spin−spin couplings. In the larger HIIs3 set we decontracted the p-shell and added three s-type primitives with large exponents to the HII basis of C and F. This was done to improve the description of the FC perturbation, which is essentially a δ function located at the nuclear site. The exponents were obtained by successive multiplication by 3, starting from the tightest s-function of the HII set. The original contraction of the other s-functions was retained, while the tight primitives were added. This represents a compromise as the full advantage of using tight functions can only be obtained with fully decontracted basis sets.[28] However, the size of $C_6H_4F_2$ would make the calculations prohibitively large using the primitive basis. The CF and FF couplings are more important than HF couplings for the present purposes; thus, we did not modify the hydrogen set in HIIs3. There are a total of 248 functions in this larger basis for $C_6H_4F_2$.

Three different MCSCF wave functions were used. The first two are of the complete active space (CAS) type,[29] ${}^{8520\ 7410}\mathrm{CAS}^{0011\ 0011}$ and ${}^{8510\ 7410}\mathrm{CAS}^{0021\ 0021}$ containing 12 and 104 Slater determinants, respectively. The third wave function is of the restricted active space (RAS) type,[30] ${}^{7410\ 6310}_{1100\ 1100}\mathrm{RAS}^{0021\ 0021}_{3200\ 3200}$. The structure of the wave function is encoded in this notation as ${}^{\mathrm{inactive}}_{\mathrm{RAS1}}\mathrm{RAS}^{\mathrm{RAS2}}_{\mathrm{RAS3}}$,[31] where the sub- and superscripts indicate the number of molecular orbitals in A_g, B_{3u}, B_{2u}, B_{1g}, B_{1u}, B_{2g}, B_{3g}, and A_u symmetry species, respectively, of the D_{2h} point group. For comparison, the SCF wave function for $C_6H_4F_2$ is ${}^{8521\ 7420}\mathrm{SCF}$. The active orbitals have been chosen on the basis of MP2 natural occupation numbers.[32]

The smallest sensible active space for this molecule, in ${}^{8520\ 7410}\mathrm{CAS}^{0011\ 0011}$, contains the highest occupied (HOMO, in the B_{3g} symmetry species) and lowest uncoccupied (LUMO, A_u) molecular orbitals, along with the occupied (B_{1g}) and unoccupied (B_{2u}) orbitals that are almost degenerate with HOMO and LUMO. In the next wave function, ${}^{8510\ 7410}\mathrm{CAS}^{0021\ 0021}$, the next occupied B_{2u} and unoccupied B_{3g} orbitals are added to the CAS space. This wave function constitutes a multireference basis, formed by the delocalized π-electron system similarly as in our earlier work for C_6H_6,[3] for our largest ${}^{7410\ 6310}_{1100\ 1100}\mathrm{RAS}^{0021\ 0021}_{3200\ 3200}$ wave function, where the maximum of two holes (particles) are allowed in the RAS1 (RAS3) subspace. While the larger of the two CAS functions is expected to cover the main part of static correlation present in the system, with the RAS function containing 389 626 determinants, we aim at estimating dynamic correlation effects to the extent that is possible using the present approach.

3. Experimental Section

p-Difluorobenzene ($C_6H_4F_2$; Fluka AG, purity > 99%) was dissolved in five LC mixtures (see Table 2).

Each sample was degassed before sealing. ^{1}H and ^{19}F NMR spectra were recorded one after another on a Bruker DSX300 at temperatures of 298, 310, and 320 K. The spectral analysis was performed on the PERCH software[33] using peak-top-fit mode in the final analysis.

The spectra are superpositions of the ones of three isotopomers: (1) those without ^{13}C, (2) those with ^{13}C bonded to hydrogen, and (3) those with ^{13}C bonded to fluorine. All of these subspectra were analyzed simultaneously. In the isotopomer 2, each hydrogen has different chemical shielding. The observable isotope shifts correlated significantly with dipolar couplings in the spectral analysis. The most reliable results were obtained by appending ^{1}H and ^{19}F spectra to the same analysis. The orientational order parameters (and geometries) of different isotopomers were the same to a good accuracy. When possible, the reported experimental *D* couplings are taken from isotopomer 2. The remaining couplings (${}^2D_{C_7H_1}$, ${}^3D_{C_7H_2}$, ${}^1D_{C_7F_6}$, and ${}^4D_{C_7F_3}$) are obtained from isotopomer 3. The spin−spin coupling constants differed to some extent from those in acetone-d_6 (20% (v/v)) and tetramethylsilane (TMS) (5% (v/v)) solution.[34] The largest solvent effects appear in couplings to fluorine (see Table 3 below). ${}^1J_{CH}$ was 164.88 Hz, whereas the present result for sample IV is 164.55 Hz. The other couplings were the same within error limits, and there was no significant variation in the *J* couplings in the various LC solvents used in the present study.

TABLE 2: Compositions of Liquid Crystal Solvents Used[a]

sample no.	liquid crystals	wt %
I	ZLI 1167	58.0
	phase IV	42.0
II	phase V	43.6
	ZLI 2806	56.4
III	EBBA[b]	35.9
	ZLI 1132	64.1
IV	ZLI 997	32.1
	ZLI 1982	67.9
V	ZLI 997	39.7
	ZLI 1167	60.3

[a] The "ZLI" and "phase" liquid crystals are products of Merck. [b] *N*-(*p*-ethoxybenzylidene)-*p*-*n*-butylaniline.

4. Results and Discussion

A. Ab Initio Calculations. The NMR spin Hamiltonian appropriate for spin = $^1/_2$ nuclei in molecules partially oriented in uniaxial LC solvents can be written in the high-field approximation as

$$\hat{H} = -B_0/(2\pi)\sum_K \gamma_K(1-\sigma_K)\hat{I}_{Kz} + \sum_{K<L} J_{KL}\hat{\mathbf{I}}_K\cdot\hat{\mathbf{I}}_L + \sum_{K<L}(D_{KL} + {}^1/_2 J_{KL}{}^{\mathrm{aniso}})(3\hat{I}_{Kz}\hat{I}_{Lz} - \hat{\mathbf{I}}_K\cdot\hat{\mathbf{I}}_L) \quad (1)$$

where B_0 is the magnetic field of the spectrometer (in the *z* direction) and γ_K, $\hat{\mathbf{I}}_K$, and σ_K are the gyromagnetic ratio, the dimensionless spin operator, and the nuclear shielding (sum of the isotropic and anisotropic contributions), of nucleus *K*, respectively. The direct dipolar coupling D_{KL} is defined as

$$D_{KL} = -\mu_0\hbar\gamma_K\gamma_L S_{KL}/(8\pi^2 r_{KL}3) \quad (2)$$

where S_{KL} is the order parameter of the internuclear vector $\mathbf{r}_{KL}$ with respect to $\mathbf{B_0}$, and μ_0 and $\hbar$ have their usual meanings. For $C_6H_4F_2$ dissolved in a uniaxial LC environment, the NMR spectra are affected by two properties of the $\mathbf{J}_{KL}$ tensors,[35] the isotropic spin−spin-coupling constant

$$J_{KL} = {}^1/_3(J_{KL,xx} + J_{KL,yy} + J_{KL,zz}) \quad (3)$$

and the anisotropic contribution

$$J_{KL}{}^{\mathrm{aniso}} = {}^2/_3 P_2(\cos\chi)\,[\Delta J_{KL}\, S_{zz}{}^D + {}^1/_2(J_{KL,xx} - J_{KL,yy})(S_{xx}{}^D - S_{yy}{}^D)] \quad (4)$$

In eq 4, $\Delta J_{KL} = J_{KL,zz} - {}^1/_2(J_{KL,xx} + J_{KL,yy})$ is the anisotropy of the tensor, $S_{\alpha\beta}{}^D$ are the components of the Saupe orientation

TABLE 3: Ab Initio Calculated and Experimental Isotropic Fluorine Spin−Spin Coupling Constants in *p*-Difluorobenzene[a]

wave function	basis	$^1J_{CF}$	$^2J_{CF}$	$^3J_{CF}$	$^4J_{CF}$	$^3J_{HF}$	$^4J_{HF}$	$^5J_{FF}$
$^{8520\ 7410}CAS^{0011\ 0011}$	HII	−234.9	69.3	−22.4	38.4	−9.7	15.6	57.3
$^{8510\ 7410}CAS^{0021\ 0021}$	HII	−201.7	48.8	−1.2	14.7	−1.8	8.4	29.0
$^{7410\ 6310}_{1100\ 1100}RAS^{0021\ 0021}_{3200\ 3200}$	HII	−174.6	40.0	3.1	7.1	1.0	6.5	21.0
$^{8520\ 7410}CAS^{0011\ 0011}$	HIIs3	−247.1	73.3	−23.1	39.8	−10.0	16.1	58.9
$^{8510\ 7410}CAS^{0021\ 0021}$	HIIs3	−212.8	52.0	−1.0	15.4	-1.9	8.7	29.8
$^{7410\ 6310}_{1100\ 1100}RAS^{0021\ 0021}_{3200\ 3200}$	HIIs3	−184.7	42.5	3.5	7.4	1.1	6.8	21.6
$^{8520\ 7410}CAS^{0011\ 0011\ b}$	HII	−221.0	64.9	−16.8	32.4	−7.4	13.7	52.4
$^{8510\ 7410}CAS^{0021\ 0021\ b}$	HII	−193.1	48.4	0.6	13.2	−0.8	7.9	28.8
$^{7410\ 6310}_{1100\ 1100}RAS^{0021\ 0021\ b}_{3200\ 3200}$	HII	−168.1	39.9	4.3	6.5	1.8	6.2	21.3
$^{8520\ 7410}CAS^{0011\ 0011\ b}$	HIIs3	−232.6	68.7	−17.2	33.6	−7.6	14.1	53.8
$^{8510\ 7410}CAS^{0021\ 0021\ b}$	IIs3	−203.6	51.4	0.8	13.9	−0.9	8.1	29.6
$^{7410\ 6310}_{1100\ 1100}RAS^{0021\ 0021\ b}_{3200\ 3200}$	HIIs3	−177.9	42.5	4.8	6.8	1.9	6.4	21.9
exptl[c]		−240.89	24.36	8.52	2.42	8.092	4.157	17.646
exptl[d]		−242.61	24.29	8.18	2.67	7.905	4.122	17.445

[a] Values in hertz at the extrapolated theoretical geometry (Table 1) unless otherwise noted. [b] At the experimental geometry of ref 25. [c] Reference 34. [d] Present experiments in sample IV at 355 K where the LC solvent appears in isotropic phase.

tensor[36] with respect to the director **n** of the LC phase, χ is the angle between **n** and the magnetic field of the spectrometer, and P_2 is the second-order Legendre polynomial. There are thus two independent order parameters, S_{zz}^D and $S_{xx}^D - S_{yy}^D$, for this symmetry, and correspondingly two combinations of $\mathbf{J}_{KL}$ tensor elements, corresponding to a single anisotropic observable.

The ab initio calculated coupling constants J_{KL} are listed in Table 3, where a comparison of results in the solution state is also made.

The reliability of the calculation of the individual tensor elements and their combinations can be largely judged on the basis of these isotropic data. From the table we are able to estimate the effect of the various computational approximations on the coupling constants. The calculations at the experimental electron diffraction geometry result in lower magnitudes of the coupling constants as compared to the extrapolated theoretical geometry, which has longer bond lengths. The relative sensitivity of the three-bond couplings is the highest. On the contrary, the effect of improving the basis set from HII to HIIs3 is seen to generally increase the magnitude of the calculated J_{KL} by 3−6%, apart from $^3J_{HF}$ and $^3J_{CF}$ whose changes are in the 10% range. As expected, the sensitivity is slightly larger the better correlated wave function approximation one uses. Finally, better correlation treatment reduces the magnitude of the couplings significantly. The effect is dramatic on the computationally difficult $^4J_{CF}$ and particularly in the three-bond coupling constants that change sign from negative to positive when going from the CAS calculations to the RAS wave function.

The comparison of theoretical and experimental spin−spin coupling constants is generally complicated by the neglect of rovibrational and environmental influences in the calculated values. However, in the current comparison these effects do not play a decisive role, but the accuracy is limited by the electronic structure calculations themselves. Typical of ab initio calculations is that their hierarchical chain of approximations allows a priori estimations of the accuracy. In this respect the RAS/HIIs3 calculations with the largest wave function and basis are the best of the current approximations. They are found to reproduce all the signs and orders of magnitude of the experimental couplings, however, underestimating the CF and HF couplings over an odd number of bonds and overestimating the corresponding couplings over an even number of bonds. Despite the oppositely directed trends produced by improving the basis set and correlation, it is difficult to give even a rough estimate of where a further improvement, if it were practical, would put the calculated results. At least the three-, four-, and five-bond coupling constants appear to be converging toward the experimental values, although very slowly in the case of the three-bond couplings.

TABLE 4: Individual Contributions to the Isotropic Fluorine Spin−Spin Coupling Constants in *p*-Difluorobenzene[a]

contribution	$^1J_{CF}$	$^2J_{CF}$	$^3J_{CF}$	$^4J_{CF}$	$^3J_{HF}$	$^4J_{HF}$	$^5J_{FF}$
FC	−210.7	50.1	6.6	4.6	3.3	7.0	11.2
SD	11.3	3.8	−2.3	4.2	−0.9	−0.1	10.8
PSO	13.8	−11.3	−0.5	−1.2	−1.3	1.2	0.7
DSO	0.9	−0.1	−0.3	−0.2	−0.1	−1.3	−1.0

[a] Values in hertz from the RAS/HIIs3 calculations at the extrapolated theoretical geometry.

The individual physical contributions to the coupling constants obtained from the RAS/HIIs3 calculation (at the extrapolated theoretical geometry) are listed in Table 4.

The FC term is seen to dominate the $^nJ_{CF}$ ($n = 1, 2, 3$) and HF couplings. $^4J_{CF}$ and $^5J_{FF}$ obtain equally important contributions from the SD mechanism. While the DSO term is generally unimportant, PSO cannot be neglected for the one- and two-bond CF couplings. The correlation trend in the coupling constants can be largely traced back to the changes (not shown) of the calculated FC contributions. The same applies to the whole effect of switching to the HIIs3 basis set. For the CF and FF couplings, parallel correlation-induced changes take place in the SD terms as well, and for $^1J_{CF}$ also in the PSO contribution. Only the FC contribution for all the couplings, SD for $^5J_{FF}$, and PSO for $^1J_{CF}$ are expected to be prone to significant further changes from the values of the Table 4, if still larger wave functions could be used.

Ab initio determination of the molecular geometry at a reliable correlated level is not straightforward for systems of the present size. We are thus forced to empirically compare the results obtained at the extrapolated theoretical geometry and an experimental one, obtained using electron diffraction.[25] Apart from $^1J_{CF}$, the agreement of all the other calculated couplings with experiment is slightly improved when the experimental geometry is used. The one-bond CF coupling appears to be an unusually difficult case, as we can by no means anticipate that it would converge toward the experimental value, −242.6 Hz, even at the experimental geometry. For this coupling, we are tempted to call upon large solvation and/or rovibrational effects to explain the present difficulties.

Disregarding the lack of quantitative agreement with experi-

TABLE 5: Ab Initio Calculated Anisotropic Properties (Anisotropies ΔJ_{KL} and Combinations $J_{KL,xx} - J_{KL,yy}$) of the Fluorine Spin−Spin Coupling Constants in *p*-Difluorobenzene[a]

wave function	basis	Δ^1J_{CF}	$^1J_{CF,xx} - {}^1J_{CF,yy}$	Δ^2J_{CF}	$^2J_{CF,xx} - {}^2J_{CF,yy}$	Δ^3J_{CF}	$^3J_{CF,xx} - {}^3J_{CF,yy}$	Δ^4J_{CF}	$^4J_{CF,xx} - {}^4J_{CF,yy}$	Δ^3J_{HF}	$^3J_{HF,xx} - {}^3J_{HF,yy}$	Δ^4J_{HF}	$^4J_{HF,xx} - {}^4J_{HF,yy}$	Δ^5J_{FF}	$^5J_{FF,xx} - {}^5J_{FF,yy}$
$^{8520\ 7410}$CAS$^{0011\ 0011}$	HII	443.8	76.9	−78.6	−83.0	76.9	88.1	−67.8	−106.1	30.0	31.3	−15.0	−20.6	−91.9	−130.0
$^{8510\ 7410}$CAS$^{0021\ 0021}$	HII	399.9	32.1	−44.4	−30.6	44.4	39.1	−31.5	−51.5	17.8	17.7	−3.4	−7.0	−48.4	−57.7
$^{7410\ 6310}$RAS$^{0021\ 0021}_{1100\ 1100}$	HII	358.4	12.1	−36.2	−19.3	36.6	28.4	−18.8	−33.5	16.0	15.1	−1.4	−4.6	−35.8	−37.2
$^{8520\ 7410}$CAS$^{0011\ 0011}$	HIIs3	456.0	78.2	−80.2	−84.5	78.7	90.0	−69.4	−108.3	29.9	31.3	−15.0	−20.7	−94.2	−132.6
$^{8510\ 7410}$CAS$^{0021\ 0021}$	HIIs3	411.1	32.2	−45.3	−30.9	45.5	40.0	−32.2	−52.5	17.8	17.8	−3.4	−7.0	−49.5	−59.0
$^{7410\ 6310}$RAS$^{0021\ 0021}_{1100\ 1100}$	HIIs3	368.8	11.5	−36.9	−19.4	37.5	29.1	−19.2	−34.0	16.0	15.1	−1.4	−4.6	−36.2	−38.1
$^{8520\ 7410}$CAS$^{0011\ 0011}$ *b*	HII	416.4	60.4	−72.8	−72.7	68.8	78.2	−58.3	−94.3	26.7	29.1	−12.6	−18.3	−84.7	−118.2
$^{8510\ 7410}$CAS$^{0021\ 0021}$ *b*	HII	380.5	24.9	−45.0	−28.8	42.6	37.6	−29.3	−49.4	16.9	17.6	−3.2	−6.7	−48.0	−56.8
$^{7410\ 6310}$RAS$^{0021\ 0021}_{1100\ 100}$ *b*	HII	342.4	6.6	−37.3	−18.3	35.5	27.6	−17.8	−32.6	15.4	15.1	−1.4	−4.4	−36.0	−37.4
$^{8520\ 7410}$CAS$^{0011\ 0011}$ *b*	HIIs3	427.9	61.4	−74.3	−73.9	70.4	79.9	−59.8	−96.3	26.6	29.2	−12.5	−18.3	−86.7	−120.6
$^{8510\ 7410}$CAS$^{0021\ 0021}$ *b*	HIIs3	391.3	24.9	−45.9	−29.1	43.6	38.5	−30.0	−50.3	16.8	17.7	−3.2	−6.7	−49.1	−58.2
$^{7410\ 6310}$RAS$^{0021\ 0021}_{1100\ 1100}$ *b*	HIIs3	352.3	6.0	−38.0	−18.4	36.3	28.3	−18.3	−33.2	15.3	15.1	−1.4	−4.4	−36.6	−38.2

[a] Values in hertz at the extrapolated theoretical geometry unless otherwise noted. The anisotropies are defined as $\Delta J = J_{zz} - {}^1/_2(J_{xx} + J_{yy})$. [b] At the experimental geometry of ref 25.

TABLE 6: Individual Contributions to the Anisotropic Properties of the Fluorine Spin−Spin Coupling Tensors in *p*-Difluorobenzene[a]

contribution	$^1\mathbf{J}_{CF}$	$^2\mathbf{J}_{CF}$	$^3\mathbf{J}_{CF}$	$^4\mathbf{J}_{CF}$	$^3\mathbf{J}_{HF}$	$^4\mathbf{J}_{HF}$	$^5\mathbf{J}_{FF}$
			ΔJ				
SD/FC	370.1	−31.7	33.7	−19.6	17.7	−2.3	−25.4
SD	34.2	−1.6	1.9	−1.8	0.1	−0.6	1.9
PSO	−59.6	−6.9	0.2	0.6	0.3	−1.3	−16.4
DSO	24.0	3.2	1.7	1.6	−2.1	2.8	3.7
			$J_{xx} - J_{yy}$				
SD/FC	26.5	−1.4	26.0	−23.4	11.0	−5.3	−31.6
SD	16.5	−7.3	4.7	−7.2	−2.3	0.2	−19.7
PSO	−31.0	−11.9	−1.6	−3.2	−1.8	−0.2	13.4
DSO	−0.5	1.2	0.1	−0.2	8.2	0.8	−0.2

[a] Values in hertz from the RAS/HIIs3 calculations at the extrapolated theoretical geometry.

ment, the qualitatively correct isotropic couplings are, for the present purposes, a strong recommendation for the quality of the calculated anisotropic properties of the coupling tensors, displayed in Table 5.

The sensitivity of the calculated anisotropies ΔJ_{KL} and the asymmetry-related combinations of the tensor elements, $J_{KL,xx} - J_{KL,yy}$, to the choice of geometry and electron correlation treatment is generally similar to that observed for the coupling constants. Exceptions to this are the parameters of the $^1\mathbf{J}_{CF}$ and $^2\mathbf{J}_{CF}$ tensors, where the anisotropic properties display larger relative changes. While improvements in the correlation treatment clearly decrease the magnitude of the properties, the better basis set gives a smaller increase, and the trends thus partially cancel. There are no sign changes in any of the anisotropic parameters. On the contrary, the effects of improving the basis set are of the same direction but smaller than for the J_{KL}, being typically of the order of 2% here. Normally the anisotropic contributions to the $\mathbf{J}_{KL}$ tensors are dominated by the SD/FC cross-term contribution. Since the basis set dependence at this level is due to the FC interaction, it is natural to expect $\mathbf{J}_{KL}{}^{FC}$ (a linear response function with the FC interactions at both nuclei) to be more sensitive to the basis than $\mathbf{J}_{KL}{}^{SD/FC}$, where the less demanding SD operator also contributes.

The individual terms that contribute to the anisotropic parameters at the RAS/HIIs3 level (at the extrapolated theoretical geometry) are listed in Table 6.

The SD/FC term is expectedly the dominating one for most of the anisotropies. Also all the other terms give sizable contributions in the case of $^1\mathbf{J}_{CF}$, and the PSO term is significant for $^5\mathbf{J}_{FF}$. For the very small Δ^4J_{HF}, the DSO contribution is larger than SD/FC. The dominance of the SD/FC mechanism is not as clear in the $J_{xx} - J_{yy}$ results. For this parameter in $^1\mathbf{J}_{CF}$, $^2\mathbf{J}_{CF}$, and $^5\mathbf{J}_{FF}$, the PSO term is significant, being for the first two tensors even larger than SD/FC. Any significant changes in the anisotropies due to improved correlation treatment and basis set are confined solely to the SD/FC term, whereas the SD contribution to $J_{xx} - J_{yy}$ is sensitive to correlation in the CF and FF couplings. Also PSO changes $^1J_{CF,xx} - {}^1J_{CF,yy}$ from one wave function to another. Nevertheless, significant further changes upon improved correlation treatment are expected only in the SD/FC terms of the anisotropic properties.

The principal components and the orientation of the principal axis system of the coupling tensors may be useful for the purposes of solid-state NMR. They are listed in Table 7, being calculated at the RAS/HIIs3 level (at the extrapolated theoretical geometry) and also graphically displayed in Figure 1.

Due to the symmetry, one of the principal axes of each tensor is perpendicular to the plane of the molecule. One of the in-

TABLE 7: Principal Values and the Orientation Angle θ of the ab Initio Fluorine Spin−Spin Coupling Tensors in *p*-Difluorobenzene[a]

component	$^1\mathbf{J}_{CF}$	$^2\mathbf{J}_{CF}$	$^3\mathbf{J}_{CF}$	$^4\mathbf{J}_{CF}$	$^3\mathbf{J}_{HF}$	$^4\mathbf{J}_{HF}$	$^5\mathbf{J}_{FF}$
J_{33}	−313.4[b]	78.8[c]	31.9[c]	30.8[b]	12.4[c]	9.6[b]	52.7[b]
J_{22}	−301.9[c]	64.5[b]	−23.5[b]	−5.4[c]	−11.8[b]	8.2[c]	14.6[c]
J_{11}	61.1	−15.8	2.2	−3.2	2.6	2.7	−2.5
θ	0.0	143.3	109.7	90.0	105.3	130.3	0.0

[a] Principal values in hertz and angles in degrees. The principal values are arranged in the order $|J_{33}| > |J_{22}| > |J_{11}|$. From the RAS/HIIs3 calculations at the extrapolated theoretical geometry. [b] The corresponding principal axis points off the plane of the molecule. [c] The angle between the corresponding principal axis and the *x* coordinate axis is specified by θ.

plane axes is directed along the line joining the two coupled nuclei for $^1\mathbf{J}_{CF}$, $^3\mathbf{J}_{CF}$, $^4\mathbf{J}_{CF}$, and $^5\mathbf{J}_{FF}$.

B. Liquid Crystal NMR Experiments. The experimentally observable anisotropic couplings can be partitioned as[2]

$$D_{KL}^{\text{exp}} = D_{KL} + {}^1/_2 J_{KL}^{\text{aniso}} = D_{KL}^{\text{eq}} + D_{KL}^{\text{h}} + D_{KL}^{\text{ah}} + D_{KL}^{\text{d}} + {}^1/_2 J_{KL}^{\text{aniso}} \quad (5)$$

where D_{KL}^{eq} corresponds to the equilibrium geometry of the molecule, D_{KL}^{h} and D_{KL}^{ah} are the contributions of the harmonic[14] and anharmonic[37] vibrations, respectively, and D_{KL}^{d} is the deformation contribution.[13] The experimental J_{KL}^{aniso} is given by the difference $J_{KL}^{\text{aniso}} = 2(D_{KL}^{\text{exp}} - D_{KL}^{\text{calc}})$, between the experimental D_{KL}^{exp} and calculated $D_{KL}^{\text{calc}} = D_{KL}^{\text{eq}} + D_{KL}^{\text{ah}} + D_{KL}^{\text{h}} + D_{KL}^{\text{d}}$ couplings. The experimental direct couplings with their error limits at 298, 310, and 320 K are given in Tables 8−10, respectively.

The HH, CH, and HF couplings, for which J_{KL}^{aniso} contributions are likely to be small in the present system, are used to determine the orientation tensor $\mathbf{S}^D$, followed by the determination of D_{CF}^{h}, D_{FF}^{h}, D_{CF}^{d}, and D_{FF}^{d} using the harmonic force field of the molecule. The force field was obtained by modifying the force field of the corresponding chlorobenzene[38,39] similarly to that in an earlier study of difluorobenzene.[40] The contributions were calculated by the MASTER program,[41] but in the present case we used it as the FMEX (Fortran-Matlab-extension) subroutine in the Matlab program.[42] This enabled direct iteration of the relevant parameters including the properties of the indirect coupling tensors. The effects due to anharmonic vibrations were taken into account by using the AVIBR program[37] modified to include also the centrifugal distortion. The reference temperature was chosen to be 300 K, and thus, the resulting experimental geometry given by the analysis is r_α at 300 K. In calculation of anharmonic contributions we used a partial cubic force field (containing the all-diagonal stretching force constants) estimated on the basis of harmonic force field with $f_{rrr} = -3af_{rr}$, where $a = 2$ Å^{-1}.[37] For $C_6H_4F_2$, we used the ΔJ_{CH} and $J_{CH,xx} - J_{CH,yy}$ terms from the previous calculations for benzene.[3] The r_{CF} bond length was fixed to the value of 1.3476 Å obtained by transforming from r_g [25] to r_α geometry. The analysis of the experimental data is not sensitive to this value, because it only fixes the size of the system.

TABLE 8: Experimental Dipolar Couplings at 298 K of *p*-Difluorobenzene Dissolved in LC Solvents[a]

coupling	sample I	sample II	sample III	sample IV	sample V
$^3D_{H1H2}$	−1383.78(3)	−1290.01(2)	−1302.875(15)	−1405.500(11)	−1342.792(11)
$^5D_{H1H4}$	−77.07(10)	−65.42(4)	−67.26(4)	−73.17(3)	−76.48(4)
$^3D_{H1F6}$	−562.26(4)	−486.180(15)	−495.53(2)	−539.32(2)	−555.394(13)
$^4D_{H1F3}$	−188.78(4)	−173.27(2)	−175.61(2)	−189.605(15)	−183.690(13)
$^4D_{H1H5}$	−63.80(10)	−46.26(4)	−48.31(4)	−53.72(2)	−64.96(4)
$^5D_{F3F6}$	−127.81(5)	−118.836(15)	−120.46(2)	−129.70(2)	−124.076(14)
$^1D_{C8H1}$	−1790.29(8)	−1518.39(6)	−1561.89(5)	−1700.84(4)	−1771.95(3)
$^2D_{C8H2}$	−466.92(10)	−429.24(9)	−435.54(5)	−470.23(3)	−454.50(4)
$^4D_{C8H4}$	−40.10(13)	−34.17(6)	−34.93(7)	−37.95(4)	−39.78(5)
$^3D_{C8H5}$	−34.96(14)	−26.38(6)	−27.38(6)	−30.36(4)	−35.58(5)
$^2D_{C8F6}$	−322.01(7)	−294.45(2)	−298.98(3)	−322.75(3)	−313.83(2)
$^3D_{C8F3}$	−99.80(6)	−92.24(2)	−93.53(3)	−100.82(3)	−96.92(2)
$^2D_{C7H1}$	−125.50(8)	−91.26(4)	−95.26(4)	−105.86(4)	−128.27(3)
$^3D_{C7H2}$	−99.40(9)	−89.78(4)	−91.31(4)	−98.81(4)	−97.24(3)
$^1D_{C7F6}$	−2101.20(6)	−1953.78(2)	−1979.75(2)	−2132.39(6)	−2039.23(2)
$^4D_{C7F3}$	−81.08(12)	−74.70(4)	−75.68(5)	−81.03(10)	−78.39(3)

[a] Values in hertz. See Table 2 for the composition of the samples.

TABLE 9: Experimental Dipolar Couplings at 310 K of *p*-Difluorobenzene Dissolved in LC Solvents[a]

coupling	sample I	sample II	sample III	sample IV	sample V
$^3D_{H1H2}$	−1274.589(12)	−1183.667(9)	−1166.291(10)	−1305.151(9)	−1234.342(9)
$^5D_{H1H4}$	−70.01(3)	−59.41(3)	−58.21(3)	−65.60(2)	−69.50(3)
$^3D_{H1F6}$	−511.330(13)	−442.183(11)	−431.777(12)	−486.335(10)	−505.363(10)
$^4D_{H1F3}$	−173.385(13)	−158.546(11)	−156.441(12)	−175.194(10)	−168.581(11)
$^4D_{H1H5}$	−56.39(4)	−41.17(3)	−39.25(3)	−44.94(2)	−57.97(3)
$^5D_{F3F6}$	−117.720(14)	−109.005(11)	−107.768(12)	−120.537(10)	−114.084(11)
$^1D_{C8H1}$	−1622.97(4)	−1376.51(3)	−1353.35(3)	−1524.33(3)	−1608.35(3)
$^2D_{C8H2}$	−429.20(4)	−393.64(3)	−388.36(4)	−434.86(3)	−417.01(3)
$^4D_{C8H4}$	−36.36(5)	−30.84(3)	−30.25(4)	−34.04(3)	−36.11(3)
$^3D_{C8H5}$	−31.15(5)	−23.37(3)	−22.50(4)	−25.64(3)	−31.79(4)
$^2D_{C8F6}$	−295.73(2)	−269.522(15)	−266.02(2)	−297.891(14)	−287.765(15)
$^3D_{C8F3}$	−91.72(2)	−84.52(2)	−83.52(2)	−93.443(14)	−89.04(2)
$^2D_{C7H1}$	−111.15(3)	−81.21(3)	−77.28(3)	−88.47(2)	−114.41(3)
$^3D_{C7H2}$	−91.14(3)	−82.07(3)	−80.97(3)	−90.74(3)	−89.05(3)
$^1D_{C7F6}$	−1934.63(2)	−1790.986(14)	−1771.42(2)	−1980.949(15)	−1873.79(2)
$^4D_{C7F3}$	−73.97(3)	−68.52(3)	−67.16(6)	−75.56(3)	−71.76(3)

[a] Values in hertz. See Table 2 for the composition of the samples.

TABLE 10: Experimental Dipolar Couplings at 320 K of *p*-Difluorobenzene Dissolved in LC Solvents[a]

coupling	sample I	sample II	sample III	sample IV	sample V
$^3D_{H1H2}$	−1155.785(10)	−1072.604(10)	−1204.129(10)	−1203.647(10)	−1106.376(10)
$^5D_{H1H4}$	−62.94(3)	−53.65(3)	−59.22(3)	−59.16(3)	−61.75(3)
$^3D_{H1F6}$	−460.029(12)	−399.649(13)	−440.735(12)	−440.557(12)	−450.273(13)
$^4D_{H1F3}$	−156.993(12)	−143.598(13)	−161.129(12)	−161.081(13)	−150.886(13)
$^4D_{H1H5}$	−49.81(3)	−36.98(3)	−38.78(3)	−38.78(3)	−51.12(3)
$^5D_{F3F6}$	−106.793(13)	−98.831(13)	−111.178(12)	−111.159(12)	−102.294(14)
$^1D_{C8H1}$	−1456.57(3)	−1242.96(4)	−1376.03(3)	−1375.39(3)	−1429.94(3)
$^2D_{C8H2}$	−388.71(3)	−356.75(4)	−400.15(4)	−400.02(4)	−373.54(3)
$^4D_{C8H4}$	−32.63(4)	−27.92(4)	−30.80(4)	−30.81(4)	−32.12(4)
$^3D_{C8H5}$	−27.66(4)	−21.06(4)	−22.32(4)	−22.24(4)	−27.99(4)
$^2D_{C8F6}$	−267.73(2)	−244.16(2)	−273.70(2)	−273.60(2)	−257.50(2)
$^3D_{C8F3}$	−83.15(2)	−76.59(2)	−86.08(2)	−86.08(2)	−79.73(2)
$^2D_{C7H1}$	−98.29(3)	−72.82(3)	−76.28(4)	−76.45(5)	−100.68(3)
$^3D_{C7H2}$	−82.36(3)	−74.36(4)	−83.12(3)	−82.92(4)	−79.57(3)
$^1D_{C7F6}$	−1754.04(2)	−1622.74(2)	−1826.82(2)	−1820.85(3)	−1678.98(2)
$^4D_{C7F3}$	−67.17(3)	−62.10(6)	−69.57(6)	−70.05(4)	−64.33(3)

[a] Values in hertz. See Table 2 for the composition of the samples.

TABLE 11: Example of Experimental, D^{exp}, and Fitted, D^{calc}, Dipolar Couplings with Different Contributions in Sample I at 320 K[a]

coupling[b]	D^{eq}	D^h	δD^{ah}	D^d	$^1/_2J_{aniso}$	D^{calc}	D^{exp}	diff
$^3D_{H1H2}$	−1171.89	17.87	−0.26	−1.51	*c*	−1155.79	−1155.79	0.00
$^5D_{H1H4}$	−63.40	0.35	−0.01	0.07	*c*	−62.99	−62.94	0.05
$^3D_{H1F6}$	−469.12	7.48	−0.10	0.30	1.40	−460.04	−460.03	0.01
$^4D_{H1F3}$	−157.73	0.89	−0.04	0.10	−0.24	−157.02	−156.99	0.03
$^4D_{H1H5}$	−50.25	0.57	−0.01	−0.08	*c*	−49.77	−49.81	−0.04
$^5D_{F3F6}$	−103.46	−0.06	−0.03	0.06	−3.30	−106.79	−106.79	0.00
$^1D_{C8H1}$	−1581.83	126.50	−0.63	0.65	−1.27	−1456.58	−1456.57	0.01
$^2D_{C8H2}$	−398.27	9.20	−0.09	−0.02	0.47	−388.72	−388.71	0.01
$^4D_{C8H4}$	−33.08	0.17	0.00	0.04	0.36	−32.52	−32.63	−0.11
$^3D_{C8H5}$	−27.73	0.26	0.00	−0.03	−0.13	−27.63	−27.66	−0.03
$^2D_{C8F6}$	−267.71	2.66	−0.06	0.29	−2.90	−267.72	−267.73	−0.01
$^3D_{C8F3}$	−84.90	0.30	−0.02	0.03	1.44	−83.15	−83.15	0.00
$^2D_{C7H1}$	−101.70	3.06	−0.02	−0.28	0.65	−98.29	−98.29	0.00
$^3D_{C7H2}$	−82.95	0.82	−0.02	0.02	−0.26	−82.38	−82.36	0.02
$^1D_{C7F6}$	−1821.11	46.74	−0.77	−2.30	23.40	−1754.04	−1754.04	0.00
$^4D_{C7F3}$	−64.88	0.09	−0.01	0.07	−2.41	−67.15	−67.17	-0.02
ΔA_{CH}[d]	0.82	η_{CH}		0.0295		S_{zz}	0.15683	
ΔA_{CF}[d]	10.38	η_{CF}		0.0252		$S_{xx} - S_{yy}$	0.22251	
ΔA_{C8C9}[d]	12.28	ΔA_{C7C8}[d]		13.15				

[a] Values in hertz. D^h is due to harmonic vibrations, $\delta D^{ah} = D^{ah}(320K) - D^{ah}(300K)$ comes from the changes in anharmonic vibrations (see eq 5) compared with the reference temperature, 300 K. D^d is due to solvent-induced deformation of molecular geometry, and $^1/_2J_{aniso}$ is the indirect part of the experimental coupling. The anisotropy and asymmetry parameters of the interaction tensor for each bond are also shown (if not zero). [b] For numbering of the atoms, see Figure 1. [c] Assumed to be zero. [d] Anisotropies in units of 10^{-22} J.

The present nematic solvent mixtures are so-called "good" mixtures, with compositions chosen particularly to minimize the anisotropic couplings of the methane probe molecule, implying minimal D_{KL}^d contribution due to anisotropic forces.[43] In the present case, the fluorine substitution makes the investigated molecule more prone to specific interactions than, e.g., hydrocarbons in general. Thus, the molecular geometry may depend on the LC solvent used, and it is not safe to constrain it to be the same in different samples. For a given sample the solvent effects are likely to be rather similar at different temperatures and the obtained data as functions of temperature are explainable with the same geometry, corrected for temperature dependent anharmonic vibrations. This means that a set of measured direct couplings using different LC solvents may demand a larger number of free parameters in the iteration procedure than in the case where one LC solvent is used at different temperatures.

The CH, CF, and CC interaction tensors, **A**, are second-rank traceless tensors for each type of chemical bond of the solute; the **A** determine the torques acting on the corresponding bonds.[11−13] The anisotropies, $\Delta A = A_{zz} - {}^1/_2(A_{xx} + A_{yy})$, and asymmetry parameters, $\eta = (A_{xx} - A_{yy})/A_{zz}$, depend on the instantaneous angle between the bond direction and the director. In the case of hydrocarbons, the tensors are often cylindrically symmetric with respect to the direction of the corresponding bond. However, the fit to the experimental data is poor unless the η parameters of the $\mathbf{A}_{CH}$ and $\mathbf{A}_{CF}$ tensors are also included. There are two distinct types of CC bonds in the molecule and the corresponding ΔA_{C7C8} and ΔA_{C8C9} were assumed to have a vanishing asymmetry parameter, $\eta = 0$, as the carbon atoms are not directly perturbed by the surrounding molecules due to the geometry of the $C_6H_4F_2$. The results of the optimization for sample I at 320 K are given as an example in Table 11.

The corrections due to deformation are small as expected. The difference between experimental and calculated couplings is generally small as compared to the indirect contributions. For $^5D_{FF}$, $^2D_{CF}$, $^3D_{CF}$, $^4D_{CF}$, and surprisingly also for $^4D_{CH}$, J_{KL}^{aniso} gives the most important contribution, whereas harmonic vibrational motion gives a slightly larger correction to $^1D_{CF}$. If we use average experimental results (for $^4D_{CH}$ the previous ab initio results in benzene) for these indirect couplings, we obtain the ratios $^1/_2J_{KL}^{aniso}/(D_{KL}^{eq} + D_{KL}^h + D_{KL}^d)$ of +3.2, +1.1, −1.7, +3.6, −1.1, and −1.2%, in the respective order of the couplings. The corresponding numbers are +3.2, +1.0, −3.6, +3.5, −1.1,

and −1.1% if the ab initio results (RAS/HIIs3/extrapolated theoretical geometry) for the **J** tensors are used. The largest $^1/_2 J_{KL}{}^{\mathrm{aniso}}$ contributions are thus found in the same couplings as pointed out in earlier work.[40] From the theoretical data, the contributions to $^3D_{\mathrm{HF}}$ and $^4D_{\mathrm{HF}}$ are −0.3 and +0.2%, respectively.

In the present case we have many observable couplings. This tends to partially compensate the errors in the resulting molecular geometry, if the indirect contributions are ignored. The effects of compensation when neglecting the CF and FF indirect contributions are clearly seen in the root mean square error of the fit, which is only 9.8 times larger than with them. Despite this, the biggest relative error due to the approximation is in the ∠C12−C7−C8 bond angle, +1.5%, which is nearly 2°. The largest deviation on the distances is in r_{C7F3}, −1.4%. In large molecules, the direct couplings to fluorine are used in determinations of molecular geometry because they are in many cases the only observable couplings. The partial error compensation in geometry is then excluded, and the indirect contributions may be even more important than in the present case. It is essential to note that the relative indirect contribution is orientation dependent because the main components (in the principal axis system) of the indirect and direct coupling tensors are often in different directions. The above numbers represent, thus, an example with one molecular orientation.

The optimized geometries of *p*-difluorobenzene in the samples are given in Table 1. The ab initio, LC, and ED geometries are not fully comparable, because the first is r_e, the second r_α, and the last r_g geometry. r_g is transformable to r_α by applying corrections due to harmonic vibrations. r_α, again, is transformable to r_e by taking anharmonic corrections into account.[37] The effect of harmonic corrections on bond lengths obtained from NMR may be several percent, whereas the typical anharmonic correction is under 0.01 Å. It means that r_α and r_e are often close to each other, while r_g may differ markedly. For this reason we have transformed the ED geometry to r_α at 300 K, which is directly comparable with the present LC results. In the present case we do not tabulate the experimental r_e geometry because the anharmonic force field used is partially incomplete. Only the estimated diagonal terms are available which, however, enable a reliable estimate for the anharmonic contributions on direct couplings in a narrow temperature range (leading to an accurate r_α geometry). We have calculated the geometries at the measurement temperatures (298, 310, and 320 K) from r_α at 300 K with the equation

$$r_\alpha(T) = r_\alpha(300\mathrm{K}) + [\delta r(T) - \delta r(300\mathrm{K})] \qquad (6)$$

where $\delta r(T) = r_\alpha(T) - r_e$ is calculated on the basis of the anharmonic force field and r_α(300K) is free in iteration (in the present case the approximate δr(300K) values are 0.0040, 0.0010, 0.0033, and 0.0033 Å and 0.17° and 0.05° for r_{CH}, r_{CF}, r_{C7C8}, and r_{C8C9} and ∠C12−C7−C8 and ∠H1−C8−C9, respectively). In LC NMR, the relative internuclear distances are obtained with respect to a chosen bond length in the analysis of the data, which does not affect the bond angles. The results for the present experiments are in good mutual agreement. If we ignore the possible solvent effects, we obtain r_{CH} = 1.0818(11) Å, r_{CF} = 1.3476 Å (fixed), r_{C7C8} = 1.3906(15) Å, r_{C8C9} = 1.3966(14) Å, ∠C12−C7−C8 = 122.00(9)° and ∠H1−C8−C9 = 121.35(3)° (standard deviations in parentheses in units of last digits). Compared with the electron diffraction results, the largest differences are in r_{CH} and ∠H1−C8−C9 which "should not be considered as well-determined" by the ED study.[25]

TABLE 12: Experimental Indirect CF and FF Coupling Tensors of *p*-Difluorobenzene[a]

property	$^1\mathbf{J}_{\mathrm{CF}}$	$^2\mathbf{J}_{\mathrm{CF}}$	$^3\mathbf{J}_{\mathrm{CF}}$	$^4\mathbf{J}_{\mathrm{CF}}$	$^5\mathbf{J}_{\mathrm{FF}}$
J[b]	−242.61	24.29	8.18	2.67	17.445
ab initio[c]	−184.7	42.5	3.5	7.4	21.6
ab initio[d]	−177.9	42.5	4.8	6.8	21.9
ΔJ[e]	400 ± 90	−39 ± 2	17.6 ± 0.2	−20.0 ± 0.9	−36.5 ± 0.5
ab initio[c]	368.8	−36.9	37.5	−19.2	−36.2
ab initio[d]	352.3	−38.0	36.3	−18.3	−36.6
$J_{xx} - J_{yy}$[e]	13 ± 3	−20.5 ± 1.1	13.7 ± 0.1	−35 ± 2	−38.4 ± 0.5
ab initio[c]	11.5	−19.4	29.1	−34.0	−38.1
ab initio[d]	6.0	−18.4	28.3	−33.2	−38.2

[a] Values in hertz. [b] See footnote *d* in Table 3. [c] From the present RAS/HIIs3 calculations at the extrapolated theoretical geometry. [d] From the present RAS/HIIs3 calculations at the experimental electron diffraction geometry. [e] Average of the present five LC NMR results. The error limits are standard deviations. The anisotropic contributions to the HF couplings and the ratios $\Delta J/(J_{xx} - J_{yy})$ for the CF and FF couplings, are taken from the ab initio calculations (RAS/HIIs3/extrapolated theoretical geometry) in the analysis of the experimental data. The indirect contributions on CH couplings are calculated on the basis of ab initio results for benzene.[3]

The $C_6H_4F_2$ solute is oriented quite strongly in the present solvents. The typical order parameters, S_{zz} = 0.16 and $S_{xx} - S_{yy}$ = 0.22 (Table 11), are large enough to allow ignoring the small solvent effects in the isotropic *J* coupling constants, which were fixed to the same values for each sample in the analysis. The contributions due to the orientation dependent anisotropic properties of the indirect fluorine couplings are larger than in the case of CC couplings in hydrocarbons[3,4] or HF, CF, and FF couplings in fluoromethanes,[19] which makes the present analysis less sensitive to noise in the data.

We were not able to extract the ΔJ_{KL} and $J_{KL,xx} - J_{KL,yy}$ elements from the experimental $J_{KL}{}^{\mathrm{aniso}}$ alone, but the analysis had to be performed by fixing the ratio $\Delta J_{KL}/(J_{KL,xx} - J_{KL,yy})$ for the CF and FF couplings to the ab initio result (RAS/HIIs3/extrapolated theoretical geometry), leaving only one adjustable parameter for each tensor. These "semiexperimental" indirect CF and FF coupling tensors are given in Table 12. The error limits are obtained from the standard deviation of the five different measurements.

The ab initio and experimental results are found to be in satisfactory agreement; the signs are consistently the same, and the experimental magnitudes are well-reproduced by the calculation. Generally, the present level of agreement of theory and experiment must, in the light of corresponding comparison to the isotropic coupling constants, be considered slightly artificial. Nevertheless, these results form a firm qualitative basis for evaluating the importance of the effects due to $J_{KL}{}^{\mathrm{aniso}}$ of the fluorine coupling tensors on the corresponding experimental anisotropic couplings.

As already stated, the relative contribution of the measured or calculated $J_{KL}{}^{\mathrm{aniso}}$ parameters entering $D_{KL}{}^{\mathrm{exp}}$ for couplings to fluorine are too large to be neglected in accurate experimental work. For molecules possessing the D_{2h} (such as the present $C_6H_4F_2$) or lower point group symmetry, the traceless and symmetric $\mathbf{S}^D$ tensor has two or more (up to five) independent elements, i.e., order parameters. Close to a certain combination of the parameters (e.g., in the present case, $\Delta D_{KL} S_{zz}{}^D = -^1/_2 (D_{KL,xx} - D_{KL,yy})(S_{xx}{}^D - S_{yy}{}^D)$, see eq 4), a situation may arise where the direct coupling contribution nearly vanishes but the indirect coupling contribution does not. Consequently, the latter may even dominate the experimental anisotropic coupling. For example, consider a situation for the present molecule in which S_{zz} is fixed to 0.3 and the ratio $^3J_{\mathrm{HF}}{}^{\mathrm{aniso}}/(2\,{}^3D_{\mathrm{HF}}{}^{\mathrm{eq}})$ is maximized by iterating $S_{xx} - S_{yy}$. Around $S_{xx} - S_{yy}$ = 0.022,

the direct coupling approaches zero and the indirect part dominates the experimental coupling. Due to the fact that the anisotropic properties of the $^3\mathbf{J}_{HF}$ tensor are small, the measured coupling is quite weak, only 1.65 Hz, calculated on the basis of the current ab initio results. However, for a slightly different choice of the parameters, $S_{zz} = 0.3$ and $S_{xx} - S_{yy} = 0.018$, the relative value of 20% for the ratio $^3J_{HF}{}^{aniso}/(2\ ^3D_{HF}{}^{eq})$ is obtained with the experimental coupling about 10 Hz. Although these order parameter values are not typical for the present disk-shaped solute (for which S_{xx} is very different from S_{yy}), they are in a fully acceptable range for general, larger LC molecules containing fluorine-substituted benzenes. Likewise, the possibility of similar cancellation of the direct couplings should be considered in biomacromolecules.

The spin−spin coupling properties are very difficult or even impossible to calculate with ab initio methods for large molecules due to computational limitations. However, if fluorine couplings are used in accurate determinations of molecular orientation and geometry, one reasonable method of estimating the indirect contribution is to calculate the necessary properties for a small model system including similar structural units. If the indirect contribution is ignored, one should, at least, ensure that there are no strong cancellations in the direct couplings with the observed orientation, leading to anomalous indirect contributions.

5. Conclusions

We have used the ab initio multiconfiguration self-consistent field linear response method to calculate the spin−spin coupling tensors, $\mathbf{J}_{XF}$ (X = H, C, F), to fluorine in *p*-difluorobenzene, serving as a prototype of fluorine-substituted aromatic systems. Three active molecular orbital spaces, two one-particle basis sets, and two molecular geometries were used to test the approximations made. All the five physical contributions to the **J** tensors were consistently calculated at each level. The best tensors are given in both molecule-fixed frame and in the principal axis system. The calculations were able to qualitatively reproduce the experimental *J* coupling constants, but the size of the system prevented definite convergence of the results. However, improved approximations lead to better agreement between theory and experiment apart from $^1J_{CF}$, where we suspect significant solvation or rovibrational effects. On the basis of the coupling constants, the calculated anisotropic properties of the coupling tensors are also expected to be qualitatively correct.

All the $^1/_2J_{XF}{}^{aniso}$ (X = C, F) contributions to the anisotropic couplings were experimentally determined using NMR of $C_6H_4F_2$ dissolved in special nematic liquid crystal solvent mixtures. The agreement with ab initio results (combined with the experimental orientation tensor of the solute) is very satisfactory, corroborating the reliability of both experimental and theoretical methods used. It was not possible to break in a unique way the $^1/_2J_{XF}{}^{aniso}$ results into contributions of the properties of the $\mathbf{J}_{XF}$ tensor, ΔJ_{XF}, and $J_{XF,xx} - J_{XF,yy}$, using the LC NMR data alone. Inserting some of the ab initio results in the analysis of the experiments, the remaining parameters were found to be in excellent agreement with the calculations.

On the basis of both theoretical and experimental findings, the contributions of the anisotropic properties of the fluorine spin−spin coupling tensors to the corresponding experimental anisotropic couplings are larger than those pertinent to CC, CH, and HH couplings. In the case of multiple order parameters, the indirect coupling can theoretically even dominate the experimental dipolar coupling because of the occasionally canceled direct part. In principle this is possible for all dipolar couplings, but because the anisotropic properties of the $\mathbf{J}_{HH}$ and $\mathbf{J}_{CH}$ tensors are small, even total cancellation of the direct part leads to very weak experimental coupling. In the case of couplings to fluorine, the indirect part can contribute significantly, around 3% in the present study, and the contribution can occasionally be much larger depending on the orientation tensor of the molecule.

Acknowledgment. The authors are grateful to the Academy of Finland for financial support. J.K. wants to express his gratitude to the Finnish Cultural Foundation and the Oulu University Foundation for grants. Dr. Päiviö Pollari is thanked for help with the Fortran-Matlab extension. Mr. Juha-Heikki Kantola is thanked for his valuable assistance with Figure 1. The computational resources were supplied by the Center for Scientific Computing, Espoo, Finland.

References and Notes

(1) Lounila, J.; Jokisaari, J. *Prog. Nucl. Magn. Reson. Spectrosc*. **1982**, *15*, 249.
(2) Jokisaari, J. In *Encyclopedia of Nuclear Magnetic Resonance*; Grant, D. M., Harris, R. K., Eds.; Wiley: Chichester, U.K. 1996; Vol. 2, p 839.
(3) Kaski, J.; Vaara, J.; Jokisaari, J. *J. Am. Chem. Soc*. **1996**, *118*, 8879.
(4) Kaski, J.; Lantto, P.; Vaara, J.; Jokisaari, J. *J. Am. Chem. Soc*. **1998**, *120*, 3993.
(5) (a) Sandström, D.; Summanen, K. T.; Levitt, M. H. *J. Am. Chem. Soc*. **1994**, *116*, 9357. (b) Sandström, S.; Levitt, M. H. *J. Am. Chem. Soc.* **1996**, *118*, 6966.
(6) Saupe, A.; Englert, G. *Phys. Rev. Lett*. **1963**, *11*, 462.
(7) Prestegard, J. H. *Nature Struct. Biol*. **1998**, *5*, 517, and references cited therein.
(8) Haigh, C. W.; Sykes, S. *Chem. Phys. Lett*. **1973**, *19*, 571.
(9) (a) Magnuson, M. L.; Tanner, L. F.; Fung, B. M. *Liq. Cryst*. **1994**, *16*, 857. (b) Magnuson, M. L.; Fung, B. M.; Schadt, M. *Liq. Cryst.* **1995**, *19*, 333.
(10) Helgaker, T.; Jaszuński, M.; Ruud, K. *Chem. Rev*. **1999**, *99*, 293.
(11) Lounila, J.; Diehl, P. *Mol. Phys*. **1984**, *52*, 827.
(12) Lounila, J.; Diehl, P. *J. Magn. Reson*. **1984**, *56*, 254.
(13) Lounila, J. *Mol. Phys*. **1986**, *58*, 897.
(14) Sýkora, S.; Vogt, J.; Bösiger, H.; Diehl, P. *J. Magn. Reson*. **1979**, *36*, 53.
(15) Vahtras, O.; Ågren, H.; Jørgensen, P.; Jensen, H. J. Aa.; Padkjær, S. B.; Helgaker, T. *J. Chem. Phys*. **1992**, *96*, 6120.
(16) Helgaker, T.; Jensen, H. J. Aa.; Jørgensen, P.; Olsen, J.; Ruud, K.; Ågren, H.; Andersen, T.; Bak, K. L.; Bakken, V.; Christiansen, O.; Dahle, P.; Dalskov, E. K.; Enevoldsen, T.; Heiberg, H.; Hettema, H.; Jonsson, D.; Kirpekar, S.; Kobayashi, R.; Koch, H.; Mikkelsen, K. V.; Norman, P.; Packer, M. J.; Saue, T.; Taylor, P. R.; Vahtras, O. DALTON, an ab initio electronic structure program, Release 1.0, 1997. See: http://www.kjemi.uio.no/software/dalton/dalton.html.
(17) Malkin, V. G.; Malkina, O. L.; Salahub, D. R. *Chem. Phys. Lett*. **1994**, *221*, 91.
(18) Malkina, O. L.; Salahub, D. R.; Malkin, V. G. *J. Chem. Phys*. **1996**, *105*, 8793.
(19) Lantto, P.; J. Kaski, J.; Vaara, J.; Jokisaari, J. Submitted for publication.
(20) Frisch, M. J.; Trucks, G. W.; Schlegel, H. B.; Gill, P. M. W.; Johnson, B. G.; Robb, M. A.; Cheeseman, J. R.; Keith, T.; Petersson, G. A.; Montgomery, J. A.; Raghavachari, K.; Al-Laham, M. A.; Zakrzewski, V. G.; Ortiz, J. V.; Foresman, J. B.; Cioslowski, J.; Stefanov, B. B.; Nanayakkara, A.; Challacombe, M.; Peng, C. Y.; Ayala, P. Y.; Chen, W.; Wong, M. W.; Andres, J. L.; Replogle, E. S.; Gomperts, R.; Martin, R. L.; Fox, D. J.; Binkley, J. S.; Defrees, D. J.; Baker, J.; Stewart, J. P.; Head-Gordon, M.; Gonzalez, C.; Pople, J. A. *Gaussian 94*, Revision B.1; Gaussian, Inc.: Pittsburgh, PA, 1995.
(21) Møller, Chr.; Plesset, M. S. *Phys. Rev*. **1934**, *46*, 618.
(22) Pople, J. A.; Binkley, S.; Seeger, R. *Int. J. Quantum Chem. Symp*. **1976**, *10*, 1.
(23) Pople, J. A.; Head-Gordon, M.; Raghavachari, K. *J. Chem. Phys*. **1987**, *87*, 5968.
(24) Dunning, T. H., Jr. *J. Chem. Phys*. **1989**, *90*, 1007.
(25) Domenicano, A.; Schultz, G.; Hargittai, I. *J. Mol. Struct*. **1982**, *78*, 97.
(26) Kutzelnigg, W.; Fleischer, U.; Schindler, M. In *NMR Basic Principles and Progress*; Diehl, P., Fluck, E., Günther, H., Seelig, J., Eds.; Springer: Berlin, 1990; Vol. *23* p 165.

(27) Huzinaga, S. *Approximate Atomic Functions*; University of Alberta: Edmonton, Canada, 1971.
(28) Helgaker, T.; Jaszuński, M.; Ruud, K.; Górska, A. *Theor. Chem. Acc.* **1998**, *99*, 175.
(29) Siegbahn, P. E. M.; Almlöf, J.; Heiberg, A.; Roos, B. O. *J. Chem. Phys.* **1981**, *74*, 2384.
(30) Olsen, J.; Roos, B. O.; Jørgensen, P.; Jensen, H. J. Aa. *J. Chem. Phys.* **1988**, *89*, 2185.
(31) Åstrand, P.-O.; Mikkelsen, K. V.; Jørgensen, P.; Ruud, K.; Helgaker, T. *J. Chem. Phys.* **1998**, *108*, 2528.
(32) Jensen, H. J. Aa.; Jørgensen, P.; Ågren, H.; Olsen, J. *J. Chem. Phys.* **1988**, *88*, 3834.
(33) Laatikainen, R.; Niemitz, M.; Weber, U.; Sundelin, J.; Hassinen, T.; Vepsäläinen, J. *J. Magn. Reson. A* **1996**, *120*, 1.
(34) Wray, V.; Ernst, L.; Lustig, E. *J. Magn. Reson.* **1977**, *27*, 1.
(35) *Nuclear Magnetic Resonance of Liquid Crystals*; Emsley, J. W., Ed.; Reidel: Dordrecht, The Netherlands, 1985.
(36) Saupe, A. *Z. Naturforsch.* **1964**, *19a*, 161.
(37) Lounila, J.; Wasser, R.; Diehl, P. *Mol. Phys.* **1987**, *62*, 19.
(38) Scherer, J. R. *Spectrochim. Acta* **1964**, *20*, 345.
(39) Scherer, J. R. *Spectrochim. Acta A* **1967**, *23*, 1489.
(40) Pulkkinen, A.; Jokisaari, J.; Väänänen, T. *J. Mol. Struct.* **1986**, *144*, 359.
(41) Wasser, R.; Kellerhals, M.; Diehl, P. *Magn. Reson. Chem.* **1989**, *27*, 335.
(42) Matlab Version 5.2.0.3084. See: www.mathworks.com.
(43) Jokisaari, J.; Hiltunen, Y. *Mol. Phys.* **1983**, *50*, 1013.